

# Imaginary action, spinfoam asymptotics and the “transplanckian” regime of loop quantum gravity

N. Bodendorfer<sup>1,\*</sup>, Y. Neiman<sup>1†</sup>

<sup>1</sup> Institute for Gravitation and the Cosmos & Physics Department,  
Penn State, University Park, PA 16802, U.S.A.

March 21, 2013

## Abstract

It was recently noted that the on-shell Einstein-Hilbert action with York-Gibbons-Hawking boundary term has an imaginary part, proportional to the area of the codimension-2 surfaces on which the boundary normal becomes null. We extend this result to first-order formulations of gravity, by generalizing a previously proposed boundary term to closed boundaries. As a side effect, we settle the issue of the Holst modification vs. the Nieh-Yan density by demanding a well-defined variational principle. We then set out to find the imaginary action in the large-spin 4-simplex limit of the Lorentzian EPRL/FK spinfoam. It turns out that the spinfoam's effective action indeed has the correct imaginary part, but only if the Barbero-Immirzi parameter  $\gamma$  is set to  $\pm i$  *after* the quantum calculation. An interpretation and a connection to other recent results is discussed. In particular, we propose that the large-spin limit of loop quantum gravity can be viewed as a high-energy “transplanckian” regime.

PACS numbers: 04.20.Fy, 04.60.Pp, 11.10.Jj

---

\*norbert@gravity.psu.edu

†yashula@gmail.com

# 1 Introduction

The verification of the correct classical limit of a theory of quantum gravity, i.e. general relativity (GR), is the most basic and commonly agreed upon requirement we demand from it. For this, it is mandatory to have a thorough understanding of the classical theory. An interesting feature of the classical Einstein-Hilbert action for general relativity, which can serve as a non-trivial test of the classical limit(s) of a quantum theory<sup>1</sup>, was recently pointed out in [1, 2]. There, it was shown that the on-shell Einstein-Hilbert action with York-Gibbons-Hawking boundary term [3, 4] for a finite region always has an imaginary part, proportional to the area of the codimension-2 surfaces where the boundary normal becomes null. The imaginary part arises from analytically continuing the normal's angle near such surfaces, which one must do to avoid a pole singularity<sup>2</sup> in the York-Gibbons-Hawking boundary integral. An imaginary action in GR has been discussed long ago by Gibbons and Hawking [4] in the context of a stationary black hole Wick-rotated to Euclidean spacetime. After correcting for an infinite constant and some terms related to conserved charges, the imaginary action of [4] yields the Bekenstein-Hawking entropy. The results of [1, 2] indicate that an imaginary part is a much more general feature of gravitational actions, and that we should look for it in the classical limits of candidate quantum gravity theories. The general study of actions in finite regions, in particular for gravity, is motivated in more detail in section 2.

In the classical limit, the (effective) on-shell action is related to transition amplitudes through the path integral formalism. Therefore, models based on path-integral quantization are well suited for testing the above-mentioned feature of the GR action. Loop quantum gravity (LQG) [6, 7] is a candidate theory of quantum gravity that comes both in a Hamiltonian formulation and in a path integral framework, known as spinfoam models. The currently most studied spinfoam models are the EPRL/FK models [8, 9] for which many results are known. We refer to [10] for a recent review. In particular, one can study “semiclassical” coherent boundary states in the limit of large spins (corresponding to large areas). In our context, then, one would like to recover the imaginary part of the GR action from the spinfoam amplitudes for such states. We consider this issue in section 4. We find that the imaginary action is indeed recovered, but only if one sets the Barbero-Immirzi parameter  $\gamma$  to  $\pm i$  at the end of the calculation. This is intriguing, since  $\gamma = \pm i$  corresponds to self-dual Ashtekar-Barbero variables. We stress, however, that setting  $\gamma$  to  $\pm i$  is a formal procedure, since there is currently no detailed understanding of the quantum theory with  $\gamma$  non-real.

On a different route, one might be worried that the boundary term, and especially its imaginary part, might depend on the precise classical formulation. In other words, the results of [1, 2] were derived in a second-order framework, while it was suggested in [5] that the boundary term for first-order formulations of general relativity would be better behaved, i.e. finite without the need for subtracting infinite counterterms. The analysis of [5] was however restricted to spatial slices, since its aim was a Hamiltonian framework. There, the time gauge (see section 3) is accessible, and the boundary term vanishes quickly enough at spacelike infinity to give only a finite contribution. On the other hand, when considering closed boundaries, the time gauge is not accessible. We thus generalize the boundary term outside the time gauge in section 3, with the result that the imaginary part of the action is also present in the first-order formulation, in agreement with the second-order result [1, 2]. The current spinfoam models are based on a

---

<sup>1</sup>A quantum field theory can have more than one classical limit. The oldest example is wave/particle duality: quantum electrodynamics can be described in one limit by a classical field, and in another limit by classical particles (photons). In section 5, we will encounter two candidate classical limits of loop quantum gravity.

<sup>2</sup>It is well known that the York-Gibbons-Hawking boundary term diverges for non-compact spatial slices; see [5] for a discussion. This divergence is however conceptually different and not the cause for the imaginary part of the action.

variation of the first-order GR action, known as the Holst action [11], from which the Ashtekar-Barbero [12, 13] variables of loop quantum gravity can be derived. Therefore, we generalize the boundary term also to this action principle. Interestingly, we find that the boundary term for the Holst modification is given by the Nieh-Yan topological density, which has been proposed as a replacement for the Holst modification [14]. The question of whether to use one or the other as a classical starting point for LQG thus attains a Solomonic resolution by demanding a well-defined variational principle.

Section 5 is devoted to discussion, focusing on the spinfoam results from section 4. We propose to view these results within a physical interpretation of the large-spin limit of LQG as a “transplanckian” high-energy regime. In this framework, we make contact between the perturbative running of  $\gamma$  in effective field theory [15] and our proposal to set  $\gamma = \pm i$  in the spinfoam calculation. We also place in this context some recent work [16, 17] on black hole entropy within loop quantum gravity. Some of the remarks we make are speculative and should be taken with due care.

## 2 Why finite regions and closed boundaries?

In field theory, one always works with some sort of boundary data. The action principle restricts us to boundaries that are closed hypersurfaces, enveloping some region of spacetime. It is often convenient to place the boundary hypersurface at asymptotic infinity, either in whole or in part. One example is the calculation of S-matrix elements, where the “in” and “out” states are given on the asymptotic boundary of Minkowski space. Another example is when the initial and final states are given on two constant-time slices. These slices intersect at spatial infinity, thus forming a closed boundary.

On the other hand, gravity actually forces us to consider physics in finite regions. This is because spacetime curvature together with causality can make asymptotic infinity inaccessible from certain locations. The prime example is an observer inside a black hole. At the cosmological scale, it appears that *all* observers are in a similar predicament, due to the universe’s accelerating expansion. In both scenarios, one encounters the notion of a finite entropy associated with the causal horizon.

Given these circumstances, it is interesting to learn about any peculiarities of field theory that are specific to finite regions with Lorentzian causality. An important source of such peculiarities is the presence of “signature-flip” surfaces. These are codimension-2 surfaces where the boundary changes its signature from spacelike to timelike (or vice versa), and momentarily becomes null. Any closed boundary must contain such surfaces. The flip surfaces may be “hidden” in topological corners, where the boundary “makes a sharp turn” in a non-differentiable manner. For example, a closed boundary composed of two spacelike hypersurfaces, one “initial” and one “final”, carries two signature flips in the corner where the two hypersurfaces intersect. See figure 1.

At corners and/or flip surfaces, some standard tools of analytical mechanics cannot be taken for granted. This is related to the fact that the boundary-value problem for hyperbolic differential equations (i.e. for Lorentzian causality) is ill-defined. As a result, the usual formalism of boundary-data variations doesn’t hold at all points of a closed boundary, but breaks down at the corners and flip surfaces. In particular, tangential and normal gradients on such surfaces cannot be treated as independent. This affects the counting of degrees of freedom, as well as the locality properties of action variations. One usually avoids these issues by keeping the boundary data on these surfaces fixed and not worrying about contributions that arise from them. This is quite natural when the surfaces are “hidden” at asymptotic infinity, where all the dynamical fields fall off. However, in the presence of gravity, this point of view becomes problematic. First,

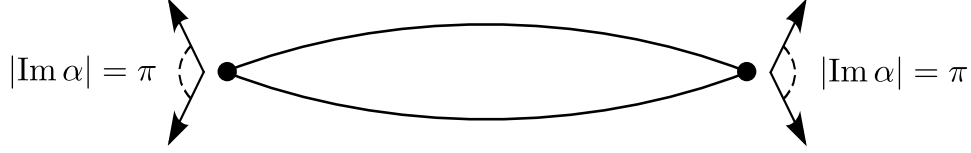


Figure 1: A purely spacelike closed boundary, composed of two intersecting hypersurfaces. The full circles denote the corner surface. The arrows indicate the two boundary normals at each intersection point. A continuous boost between these two normals involves two signature flips. As a result, the “corner angle” has an imaginary part with magnitude  $\pi$ .

as mentioned above, asymptotic infinity may be physically inaccessible. Second, the boundary’s metric and extrinsic curvature are now dynamical variables, and their values at infinity contribute to the action. This is the source of the divergence mentioned in footnote 2.

Thus, we are interested in studying actions in finite spacetime regions with an emphasis on the effects of corners and flip surfaces. The hope is to learn from this something about the degrees of freedom of quantum gravity in such regions. In [1], this approach was followed for the case of closed null boundaries. From the perspective presented above, this is an extreme case, since the boundary is null not just on isolated surfaces, but everywhere. It was noticed in [1] that for GR in a null-bounded region, a careful evaluation of the action  $S$  reveals an *imaginary part*. This conclusion was extended to general closed boundaries in [2]. The imaginary part arises from the action’s boundary term, which requires analytical continuation in the vicinity of a flip surface. Its value closely resembles the black hole entropy formula, and can be written as:

$$\text{Im } S = \frac{1}{4} \sum_{\text{flips}} \sigma_{\text{flip}} = \frac{1}{16G} \sum_{\text{flips}} A_{\text{flip}} . \quad (2.1)$$

Here, the sum is over flip surfaces,  $A_{\text{flip}}$  is the area of each surface, and  $\sigma_{\text{flip}}$  is the entropy functional  $A/4G$  [18]. The calculation was also extended to Lovelock gravity, using the action with the appropriate boundary term [19]. This resulted again in an imaginary part  $\text{Im } S$ , related in the same way as in (2.1) to the appropriate entropy formula [20]. We note again the similarity to Gibbons’ and Hawking’s calculation [4], where black hole entropy was derived from an imaginary action. The motivation there, however, was somewhat different. A Wick rotation was performed to avoid the physical singularity in the black hole’s interior. As a result, the calculation was restricted to stationary spacetimes, and did not involve finite regions.

### 3 Boundary terms in first order general relativity

#### 3.1 Second order boundary term

It is well-known that the Einstein-Hilbert action of GR must be supplemented with the York-Gibbons-Hawking boundary term [3, 4] to ensure a well-defined variational principle. The resulting action reads:

$$S_{\text{2nd-order}} = \frac{1}{16\pi G} \left( \int_{\Omega} \sqrt{-g} R d^4x + 2 \int_{\partial\Omega} \sqrt{\frac{-h}{n \cdot n}} K d^3x \right) . \quad (3.1)$$

Here,  $\Omega$  is a spacetime region with boundary  $\partial\Omega$ .  $g_{\mu\nu}$  is the space-time metric, with signature  $(-, +, +, +)$ .  $R = R^{\mu\nu}{}_{\mu\nu}$  is the Ricci scalar, with the sign convention  $R^{\mu}{}_{\nu\rho\sigma} V^{\nu} = [\nabla_{\rho}, \nabla_{\sigma}] V^{\mu}$  for the Riemann tensor  $R^{\mu}{}_{\nu\rho\sigma}$ .  $h_{ab}$  is the metric induced on  $\partial\Omega$ .  $K$  is the trace of the extrinsic

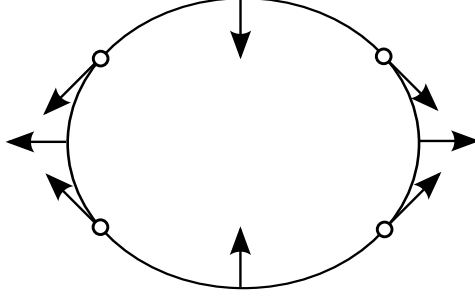


Figure 2: A smooth closed boundary in Lorentzian spacetime. The arrows indicate the normal direction at various points. The normal's sign is chosen so that it has a positive scalar product with outgoing vectors. Empty circles denote “signature flips”, where the normal becomes momentarily null.

curvature tensor  $K_a^b = \nabla_a n^b$ . The sign of the boundary normal  $n^\mu$  is chosen so that the *covector*  $n_\mu$  is outgoing, i.e. so that  $n^\mu$  has positive scalar product with outgoing vectors. See figure 2. The factor of  $n \cdot n$  in the denominator makes (3.1) valid for both spacelike and timelike patches of  $\partial\Omega$  and for arbitrary norm of  $n^\mu$ . Null regions are dealt with via an analytic continuation.  $(\mu, \nu \dots)$  are spacetime tensor indices, while  $(a, b \dots)$  are tensor indices on  $\partial\Omega$ .

Thanks to the boundary term, the action (3.1) contains only first derivatives. It is then stationary under the Einstein equations with  $\delta g_{\mu\nu} = 0$  on  $\partial\Omega$ , without also fixing  $\delta(\partial_\rho g_{\mu\nu})$ . In addition, it's worth noting that a canonical analysis of the action (3.1) leads to the ADM energy and momentum [21] as the boundary terms of the Hamiltonian and spatial diffeomorphism constraints. A recent review of these results with extensions to  $f(R)$  theories can be found in [22].

### 3.2 Gauge-invariant boundary term for the Palatini action

While the above considerations are in a second-order framework, general relativity can be equivalently described by the Palatini action, where one varies the co-vierbein  $e_\mu^I$  and the  $\text{SO}(1,3)$ -connection  $A_{\mu IJ}$  independently, thus having a first-order framework. On spacelike patches of the boundary which allow for the time gauge  $n^\mu e_\mu^I =: n^I = (1, 0, 0, 0)$ , where  $n^\mu$  is the unit normal on  $\partial\Omega$ , one can use in this gauge the action principle (see e.g. [5]):

$$\tilde{S} = \frac{1}{16\pi G} \left( \int_{\Omega} \Sigma^{IJ} \wedge F_{IJ}(A) - \int_{\partial\Omega} \Sigma^{IJ} \wedge A_{IJ} \right), \quad (3.2)$$

where  $F_{IJ}(A) := dA_{IJ} + A_I^K \wedge A_{KJ}$  is the field strength of  $A_{IJ}$ , and  $\Sigma^{IJ} := \frac{1}{2}\epsilon^{IJKL}e_K \wedge e_L$ . Our convention for the components of differential forms is  $(U \wedge V)_{\mu\nu} = 2U_{[\mu}V_{\nu]}$ . The spacetime Levi-Civita density is  $\epsilon^{\mu\nu\rho\sigma}$ , with inverse  $\epsilon_{\mu\nu\rho\sigma}$ . For the boundary, we have likewise  $\epsilon^{abc}$  and  $\epsilon_{abc}$ . The internal Levi-Civita tensor is  $\epsilon^{IJKL}$  or  $\epsilon_{IJKL}$ ; the two versions are related through raising and lowering with the flat metric  $\eta_{IJ}$ , and are *minus* each other's inverses. We assume for now that the vierbein has a positive determinant  $\det e = (1/4!)\epsilon^{\mu\nu\rho\sigma}\epsilon_{IJKL}e_\mu^I e_\nu^J e_\rho^K e_\sigma^L > 0$ . This assumption can be thought of as  $\epsilon_{\mu\nu\rho\sigma}$  and  $\epsilon_{IJKL}$  “having the same sign”. The case of negative  $\det e$  will be discussed in section 3.5.

It was shown in [5] that in the time gauge, the action (3.2) reduces to the second-order action (3.1) with the York-Gibbons-Hawking boundary term. While the time gauge is an admissible gauge choice when working on a spatial hypersurface as in the Hamiltonian framework, this gauge is not accessible everywhere on a closed boundary  $\partial\Omega$ , due to the presence of signature-

flip surfaces (section 2). For instance, in figure 1, a gauge frame with  $n^I = (1, 0, 0, 0)$  at both the initial and final hypersurfaces would fail to be continuous at the corner.

In order to see how this affects the boundary term, we must redo the calculation leading to (3.2) without the time gauge. We also leave the norm of  $n^I$  unrestricted. This will allow it to remain smooth in the neighborhood of a smooth flip surface, i.e. a signature-flip surface which is not a topological corner. Any vector  $n^I$  normal to the boundary must be collinear with the densitized quantity:

$$N_I := \frac{1}{3!} \epsilon^{abc} \epsilon_{IJKL} e_a^J e_b^K e_c^L . \quad (3.3)$$

This densitized normal  $N_I$  is a polynomial function of the co-vierbein, and it remains smooth in the vicinity of a flip surface.  $e_a^I$  in (3.3) is the pullback of the space-time co-vierbein. We define the relative sign of  $\epsilon^{abc}$  and  $\epsilon^{\mu\nu\rho\sigma}$  such that  $\epsilon_{\mu abc} \epsilon^{abc}$  has a positive scalar product with outgoing vectors. As in section 3.1, we impose the same restriction on the sign of  $n_\mu$ , which in turn determines the sign of  $n^I$ . The direction of both the densitized normal (3.3) and the undensitized normal  $n^I$  is then as depicted in figure 2. The relation between the two normals, for  $n^I$  of arbitrary length, can be expressed as:

$$N_I = \sqrt{\frac{-h}{n \cdot n}} n_I , \quad (3.4)$$

where  $h$  is the determinant of the boundary metric  $h_{ab} = e_a^I e_{bI}$ . We will also make use of the following identities:

$$\overleftarrow{\Sigma}^{IJ} = \frac{2}{n \cdot n} n^K n^{[I} \overleftarrow{\Sigma}_{K}^{J]} \quad (3.5)$$

$$\epsilon^{abd} \overleftarrow{\Sigma}_{ab}^{IJ} e_{cJ} = 2\delta_c^d N^I . \quad (3.6)$$

Eq. (3.5) expresses the fact that the pullback of  $\Sigma^{IJ}$  to the boundary always has one index normal to the boundary. Eq. (3.6) follows from symmetry, with the scalar coefficient determined by tracing the two sides.

We now set out to evaluate the boundary term in (3.2) on-shell in terms of the normal  $n^I$  (or  $N^I$ ) and the extrinsic curvature. First, we note that on-shell, the connection  $A_{IJ}$  is identified with the space-time spin connection  $\Gamma_{IJ}$  annihilating the vierbein. In coordinates, it is given by:

$$\Gamma_{\mu IJ} = e_{\nu[I} \partial_\mu e_{J]}^\nu + \Gamma_{\mu\nu}^\rho e_{[J}^\nu e_{\rho I]} , \quad (3.7)$$

where  $\Gamma_{\mu\nu}^\rho$  are the Christoffel symbols. To evaluate the boundary term in (3.2) on-shell, we write the pullback of  $\Gamma_{IJ}$  to the boundary as:

$$\overleftarrow{\Gamma}_{IJ} = \Gamma_{IJ}^H - \frac{2}{n \cdot n} n_{[I} K_{J]} . \quad (3.8)$$

Here,  $K^I$  is the 1-form  $K_a^I := e_b^I K_a^b$ , with  $K_a^b$  the extrinsic curvature from section 3.1.  $\Gamma_{IJ}^H$  is the Peldan hybrid connection [23]:

$$\Gamma_{aIJ}^H = \frac{1}{n \cdot n} n_{[I} \partial_a n_{J]} + h^{bc} (e_{b[I} \partial_a e_{cJ]} + \Gamma_{ab}^d e_{d[I} e_{cJ]}) , \quad (3.9)$$

where  $h^{ab}$  is the inverse of the boundary metric  $h_{ab}$ , and  $\Gamma_{ab}^c$  are the Christoffel symbols defined by  $h_{ab}$ . As in section 3.1, the  $n \cdot n$  factors ensure that our equations are valid for both spacelike

and timelike boundary patches, and with no restriction on the norm of  $n^I$ . The hybrid connection  $\Gamma_{IJ}^H$  has the property:

$$D_a e_b^I := \nabla_a e_b^I + \Gamma_a^{HI} J e_b^J := \partial_a e_b^I - \Gamma_{ab}^c e_c^I + \Gamma_a^{HI} J e_b^J = 0 . \quad (3.10)$$

Since the densitized normal  $N^I$  is a function of  $e_a^I$ , and  $n^I$  is collinear with  $N^I$ , we then have:

$$D_a N^I = 0; \quad n^{[I} D_a n^{J]} = 0 , \quad (3.11)$$

where  $D_a$  is again the covariant derivative defined with  $\Gamma_{ab}^c$  and  $\Gamma_a^{HI} J$ :

$$\begin{aligned} D_a N^I &:= \partial_a N^I - \Gamma_{ab}^b N^I + \Gamma_a^{HI} J N^J \\ D_a n^I &:= \partial_a n^I + \Gamma_a^{HI} J n^J . \end{aligned} \quad (3.12)$$

From (3.11)-(3.12), it follows that:

$$dn_I + \Gamma_{IJ}^H n^J \propto n_I . \quad (3.13)$$

Imposing the equation of motion  $A_{IJ} = \Gamma_{IJ}$ , we can now rewrite the boundary integral in (3.2) using eqs. (3.8), (3.5) and (3.13):

$$\begin{aligned} \int_{\partial\Omega} \Sigma^{IJ} \wedge \Gamma_{IJ} &= \int_{\partial\Omega} \frac{2}{n \cdot n} n^K n^{[I} \Sigma_K^{J]} \wedge \left( \Gamma_{IJ}^H - \frac{2}{n \cdot n} n_{[I} K_{J]} \right) \\ &= \int_{\partial\Omega} \frac{2}{n \cdot n} n_K \Sigma^{KJ} \wedge (dn_J - K_J) . \end{aligned} \quad (3.14)$$

The first term vanishes in time gauge, where  $dn^I = 0$ . The second term reproduces the York-Gibbons-Hawking integral. To see this, we restore tensor indices in the second term and use eqs. (3.6) and (3.4):

$$\begin{aligned} \int_{\partial\Omega} \Sigma^{IJ} \wedge \Gamma_{IJ} &= 2 \int_{\partial\Omega} \Sigma^{IJ} \wedge \frac{n_I dn_J}{n \cdot n} - \int_{\partial\Omega} \frac{1}{n \cdot n} n_I \epsilon^{abd} \Sigma_{ab}^{IJ} K_d^c e_{cJ} d^3x \\ &= 2 \left( \int_{\partial\Omega} \Sigma^{IJ} \wedge \frac{n_I dn_J}{n \cdot n} - \int_{\partial\Omega} \frac{n \cdot N}{n \cdot n} K d^3x \right) \\ &= 2 \left( \int_{\partial\Omega} \Sigma^{IJ} \wedge \frac{n_I dn_J}{n \cdot n} - \int_{\partial\Omega} \sqrt{\frac{-h}{n \cdot n}} K d^3x \right) \end{aligned} \quad (3.15)$$

To construct the  $d^3x$  integral in the first line, we contracted the form indices with  $\epsilon^{abc} d^3x$ , and divided by 2 due to the presence of the rank-2 form  $\Sigma^{IJ}$ .

We have thus related on-shell the boundary terms in the first-order action (3.2) and in the second-order action (3.1). It is well-known that the bulk terms of the two actions agree, given our assumption  $\det e > 0$ . We find that on-shell, the two actions are related as:

$$\tilde{S} = S_{\text{2nd-order}} - \frac{1}{8\pi G} \int_{\partial\Omega} \Sigma^{IJ} \wedge \frac{n_I dn_J}{n \cdot n} . \quad (3.16)$$

We see that in time gauge, the two actions agree. On the other hand, since  $S_{\text{2nd-order}}$  is gauge-invariant, we see that  $\tilde{S}$  is only gauge invariant under transformations that preserve the time gauge. We are thus lead to propose a modification of the boundary term:

$$S = \frac{1}{16\pi G} \left( \int_{\Omega} \Sigma^{IJ} \wedge F_{IJ}(A) - \int_{\partial\Omega} \Sigma^{IJ} \wedge \left( A_{IJ} - \frac{2N_I dN_J}{N \cdot N} \right) \right) \quad (3.17)$$

$$= \frac{1}{16\pi G} \left( \int_{\Omega} \Sigma^{IJ} \wedge F_{IJ}(A) - \int_{\partial\Omega} \Sigma^{IJ} \wedge \left( A_{IJ} - \frac{2n_I dn_J}{n \cdot n} \right) \right) . \quad (3.18)$$



On-shell, it follows from (3.16) that this modified action coincides with the second-order action (3.1). In particular, the modified boundary term in (3.17)-(3.18) coincides on-shell with the York-Gibbons-Hawking term. Off-shell, we see from (3.15) that the boundary integrals in (3.17)-(3.18) and (3.1) are related as:

$$\int_{\partial\Omega} \Sigma^{IJ} \wedge \left( A_{IJ} - \frac{2n_I dn_J}{n \cdot n} \right) = -2 \int_{\partial\Omega} \sqrt{\frac{-h}{n \cdot n}} K d^3x + \int_{\partial\Omega} \Sigma^{IJ} \wedge (A_{IJ} - \Gamma_{IJ}) \quad (3.19)$$

Both terms on the RHS are gauge-invariant (note that  $A_{IJ} - \Gamma_{IJ}$  is covariant, unlike  $A_{IJ}$  and  $\Gamma_{IJ}$  themselves). We conclude that the boundary term in the new action (3.17)-(3.18), and therefore the action itself, is gauge-invariant off-shell.

The two expressions (3.17)-(3.18) each have their advantages. The expression (3.18) involves an undensitized normal  $n^I$ , and is thus easier to interpret geometrically. On the other hand, since  $n^I$  is not constrained to unit norm, it is not a proper function of the co-vierbein. The functional structure is clearer in (3.17), which is written explicitly in terms of the connection  $A_{IJ}$  and polynomial functions ( $\Sigma^{IJ}, N_I$ ) of the co-vierbein  $e^I$ . The  $N \cdot N$  factor in the denominator in (3.17) shows that the new boundary term is non-polynomial in  $e^I$ . This is the price we pay for gauge invariance throughout a closed boundary. On the bright side, the new non-polynomial term in (3.17)-(3.18) depends only on the boundary value of  $e^I$  (through  $\Sigma^{IJ}$  and  $N_I$ ). Thus, it does not spoil the polynomial nature of the equations of motion. More generally, the action variation with fixed boundary values of  $e^I$  remains unchanged.

At a signature-flip surface, where the boundary becomes momentarily null, the  $N \cdot N$  in the denominator in (3.17) vanishes. This means that the boundary integral in (3.17)-(3.18) must be regularized. This is the same situation that was studied for the York-Gibbons-Hawking boundary term in [1, 2]. Let us now briefly review how the analysis in [1, 2] relates to our modified Palatini action (3.17)-(3.18).

### 3.3 Implications of the new Palatini boundary term

We have seen that the new  $n_I dn_J / (n \cdot n)$  term in the action (3.17)-(3.18) cancels the difference between the first-order action (3.2) and the second-order action (3.1). Let us examine some implications of this, with an emphasis on the behavior at corners and flip surfaces.

First, consider flat spacetime. There, one can choose coordinates and a gauge frame such that  $e_\mu^I = \text{const}$  and  $A_\mu^{IJ} = 0$ . In this frame, the action (3.2) for any region vanishes. On the other hand, the new term in (3.17)-(3.18) does not vanish. In fact, eq. (3.16) implies that the new term precisely captures the York-Gibbons-Hawking contribution from the boundary's extrinsic curvature. In particular, for regions  $\Omega$  that are effectively 1+1-dimensional (say, the other two dimensions form a flat torus), the on-shell action reads:

$$S = \frac{1}{8\pi G} \int_{\partial\Omega} \Sigma^{IJ} \wedge \frac{n_I dn_J}{n \cdot n} = \frac{1}{8\pi G} \int_{\partial\Omega} \sqrt{\frac{-h}{n \cdot n}} K d^3x = \frac{A}{8\pi G} \int d\alpha. \quad (3.20)$$

Here,  $d\alpha$  is the normal's rotation angle (actually, boost parameter) in the 1+1d space, while  $A$  is the area of the two transverse dimensions. To see this, it might be helpful to rewrite  $K$  as  $e^{aI} \partial_a n_I$  in the case of flat space, where  $e^{aI} := h^{ab} e_{bI}$ .

The example of an effectively 1+1d region in flat spacetime is less artificial than it may seem. In particular, it applies in the infinitesimal neighborhood of a corner surface. This is because the boundary's extrinsic curvature in the orthogonal 1+1d plane is arbitrarily larger than the gradients of  $e^I$  or the components of  $A_{IJ}$  (provided a smooth gauge frame in the spacetime). Therefore, the flat 1+1d discussion captures the fate of the ‘‘corner contributions’’ [24] to the



York-Gibbons-Hawking boundary term. We see that the corner contributions are absent in the original first-order action (3.2), and appear in the modified action (3.17)-(3.18) through the new  $n_I dn_J / (n \cdot n)$  term.

Now, as explained in [2], the signature-flip surfaces on  $\partial\Omega$  behave like corners, whether or not they coincide with corners in the topological sense. The “corner contribution” from these surfaces is responsible for the imaginary part (2.1) of the on-shell action. We see that this imaginary part is again absent in the action (3.2), and is restored in (3.17)-(3.18) through the new term.

### 3.4 Holst action

The Palatini action can be supplemented by the so-called Holst modification [11] without changing the equations of motion. Together with the appropriate boundary term, the action then reads:

$$S = \frac{1}{16\pi G} \left( \int_{\Omega} \Sigma^{IJ} \wedge F_{IJ}(A) - \int_{\partial\Omega} \Sigma^{IJ} \wedge \left( A_{IJ} - \frac{2N_I dN_J}{N \cdot N} \right) \right) + \frac{1}{16\pi G \gamma} \left( \int_{\Omega} e^I \wedge e^J \wedge F_{IJ}(A) - \int_{\partial\Omega} e^I \wedge (e^J \wedge A_{IJ} - de_I) \right), \quad (3.21)$$

where  $\gamma$  is a real nonzero constant. The first line is our modified Palatini action (3.17), while the second line describes the Holst modification. In the latter, we include the appropriate boundary integral along with the usual bulk term. The  $e^I \wedge e^J \wedge A_{IJ}$  term in the boundary integral performs the same function as the  $\Sigma^{IJ} \wedge A_{IJ}$  term in the first line - it ensures that the action variation vanishes for vanishing  $\delta e^I$  but arbitrary  $\delta A_{IJ}$  on the boundary. The  $e^I \wedge de_I$  term then performs the same function as the  $N_I dN_J / (N \cdot N)$  term in the first line - it restores full gauge invariance. This follows from the fact that the combination  $de_I - e^J \wedge A_{IJ} = de_I + A_I{}^J \wedge e_J$  is a covariant derivative. Like the  $N_I dN_J / (N \cdot N)$  term, the  $e^I \wedge de_I$  term depends only on the boundary value of  $e^I$ , and therefore doesn't enter the action variation when this boundary value is held fixed. *Unlike* the  $N_I dN_J / (N \cdot N)$  term, the  $e^I \wedge de_I$  term is polynomial in  $e^I$ . It doesn't diverge at corners or flip surfaces, and doesn't require any analytical continuation.

It is easy to see that the on-shell action is unaffected by the addition of the Holst modification. Under the equation of motion  $A_{IJ} = \Gamma_{IJ}$ , both the bulk and boundary integrands in the second line of (3.21) vanish, due to the identities:

$$e^J \wedge \Gamma_{IJ} - de_I = 0; \quad e^J \wedge F_{IJ}(\Gamma) = 0. \quad (3.22)$$

The first equation in (3.22) is the defining property of the spin connection  $\Gamma_{IJ}$ , while the second is the Bianchi identity. We conclude that on-shell, the Holst action (3.21) coincides with the modified Palatini action (3.17), and therefore also with the second-order action (3.1).

The Holst modification does have an effect on the Hamiltonian formalism. A canonical analysis of the Holst action (3.21) leads to the Ashtekar-Barbero variables [12, 13], with  $\gamma$  as the Barbero-Immirzi parameter. From a Hamiltonian point of view, different values of  $\gamma$  amount to canonical transformations [13].

While  $\gamma$  does not affect the physics at the classical level, it becomes important in loop quantum gravity [6, 7], where it appears as a quantization ambiguity. Here, the canonical transformation describing a change of  $\gamma$  cannot be implemented on the holonomy-flux algebra (see, e.g., [7]), which leads to unitarily inequivalent quantum theories [25].  $\gamma$  can thus enter the spectra of physical observables [26], and predictions of the quantum theory can depend on it.

It has been debated in the literature [14, 27, 28] whether one should use the Nieh-Yan topological density  $d(e^I \wedge T_I)$  with  $T^I := de^I + A^I{}_J \wedge e^J$  instead of the Holst modification as

the classical starting point for loop quantum gravity. The argument in favor of the Nieh-Yan density is that because it's truly topological, it does not affect the fermion coupling in the Lagrangian. As a result, the theory with fermions remains insensitive to the Barbero-Immirzi parameter at the classical level. However, our analysis above shows that to have a well-defined variational principle with arbitrary  $\delta A^{IJ}$  on the boundary, one must use a combination of the Holst and Nieh-Yan terms given in (3.21). This subtlety will also be important when discussing the running of the Barbero-Immirzi parameter, since prefactors of topological terms, e.g. the  $\theta$ -angle in QCD, are not expected to run in perturbation theory.

As a side remark, the action (3.21) can be written in a manifestly dual way as<sup>3</sup>

$$S = -\frac{1}{16\pi G} \int_{\Omega} \left( \frac{1}{2} \epsilon^{IJKL} e_K \wedge e_L + \frac{1}{\gamma} e^I \wedge e^J \right) \wedge F_{IJ}(A) \\ - \frac{1}{16\pi G} \int_{\partial\Omega} \left( \frac{1}{2} \epsilon^{IJKL} e_K \wedge e_L + \frac{1}{\gamma} e^I \wedge e^J \right) \wedge (A_{IJ} - \Gamma_{IJ}^H), \quad (3.23)$$

where  $\Gamma_{IJ}^H$  is the Peldan hybrid connection (3.9) (note that  $\Gamma_{IJ}^H$  is a functional of the  $e^I$  alone).

### 3.5 The first-order action for negative $\det e$

In the above calculations, we've been assuming  $\det e > 0$ . Let us now consider the action's behavior when both signs of  $\det e$  are allowed. This will be relevant to the spinfoam results in section 4. We build here on the discussion in [29]. Note that the sign of  $\det e$  encodes the orientation of the internal space with respect to the spacetime manifold. Thus, changing this sign can be viewed as a parity or time-reversal transformation.

When  $\det e$  changes sign, both the bulk and boundary terms in the action (3.17)-(3.18) acquire a sign factor. Thus, for  $\det e < 0$ , the real part of the first-order action (3.17)-(3.18) evaluates on-shell to *minus* that of the second-order action (3.1). As for the imaginary part, recall that its sign is determined by a choice between two complex-conjugate analytical continuations of the boundary normal's angle [1, 2]. The requirement that quantum amplitudes  $e^{iS} \sim e^{-\text{Im } S}$  do not explode exponentially forces us to choose a positive  $\text{Im } S$ , regardless of the sign of  $\det e$ . Thus, the relative sign between the real and imaginary parts of the boundary term, i.e. the choice of analytical continuation, must be different for  $\det e > 0$  and for  $\det e < 0$ .

Alternatively, one can multiply the action (3.17)-(3.18) by a factor of  $\text{sign}(\det e)$  (in the classical theory, this sign will be constant everywhere, assuming that  $\det e$  doesn't vanish):

$$S' = \frac{\text{sign}(\det e)}{16\pi G} \left( \int_{\Omega} \Sigma^{IJ} \wedge F_{IJ}(A) - \int_{\partial\Omega} \Sigma^{IJ} \wedge \left( A_{IJ} - \frac{2N_I dN_J}{N \cdot N} \right) \right). \quad (3.24)$$

The action (3.24) is invariant under changes to  $\text{sign}(\det e)$ , and its real part always evaluates on-shell to the second-order action (3.1). As a result, the same analytical continuation gives a positive  $\text{Im } S'$  for both signs of  $\det e$ . The price we pay is that the action functional (3.24) is no longer fully analytical in the vierbein. The sign function in (3.24) can be analytically continued either from positive  $\det e$  or from negative  $\det e$ . The two continuations give the constant functions  $\text{sign}(\det e) = 1$  and  $\text{sign}(\det e) = -1$ , thus forming two separate analytical domains. We see that there is a tradeoff in terms of analyticity. For the action (3.17)-(3.18), different signs of  $\det e$  require different analytical continuations for the normal's angle. On the other hand, with the action (3.24), we must contend with the two separate analytical domains of the sign function  $\text{sign}(\det e)$  itself.

---

<sup>3</sup>This observation is due to Andreas Thurn (private communication).

The appearance of two analytical domains is related to the 4-volume density  $\sqrt{-g}$  in the second-order action<sup>4</sup>. In terms of the vierbein, we have  $g = -(\det e)^2$ , and therefore:

$$\sqrt{-g} = \sqrt{(\det e)^2} = \text{sign}(\det e) \cdot \det e . \quad (3.25)$$

While (3.25) shows where the non-analytical factor of  $\text{sign}(\det e)$  comes from, it is instructive to consider the function  $\sqrt{(\det e)^2}$  in its own right. The square-root function has a branch cut induced by the choice  $\sqrt{-1} = \pm i$ . This means that a half-line, e.g.  $e^{i\theta}\mathbb{R}^+$  for some angle  $\theta \neq \pi$ , must be removed from its domain. For the function  $\sqrt{(\det e)^2}$ , this implies removing from the complex  $\det e$  plane a whole line containing  $\det e = 0$ , e.g.  $e^{i\theta/2}\mathbb{R}$ . This line splits the complex plane into two separate domains, one containing the positive half of the real line, and the other containing the negative half.

Similar considerations apply to the Holst action (3.21). Under a change in  $\text{sign}(\det e)$ , the first line in (3.21) changes sign, while the second line (the  $1/\gamma$  term) is invariant. Since the second line vanishes on-shell, the comparison with the second-order action and the choice of analytical continuation for the angle play out as before. The analogue of the action (3.24) reads:

$$\begin{aligned} S' = & \frac{\text{sign}(\det e)}{16\pi G} \left( \int_{\Omega} \Sigma^{IJ} \wedge F_{IJ}(A) - \int_{\partial\Omega} \Sigma^{IJ} \wedge \left( A_{IJ} - \frac{2N_I dN_J}{N \cdot N} \right) \right) \\ & + \frac{1}{16\pi G\gamma} \left( \int_{\Omega} e^I \wedge e^J \wedge F_{IJ}(A) - \int_{\partial\Omega} e^I \wedge (e^J \wedge A_{IJ} - de_I) \right) . \end{aligned} \quad (3.26)$$

The action (3.26) is invariant under changes to  $\text{sign}(\det e)$  and reduces on-shell to the second-order action (3.1) for both signs of  $\det e$ . As in (3.24), the price is the appearance of an explicit sign function, which splits the complex plane into two analytical domains. This action was proposed in [29] as the basis of a modified spinfoam model that would be invariant under parity and time reversal. A similar proposal was made in [30, 31], with the purpose of improving the large-spin behavior in the Euclidean model. In the Lorentzian, such modified spinfoam models have not yet been studied in detail. In section 4, we will discuss the original Lorentzian EPRL/FK spinfoams based on the action (3.21).

## 4 The imaginary action in spinfoam asymptotics

### 4.1 Introduction

We have seen that various formulations of the GR action possess an imaginary part (2.1) when supplemented with a gauge-invariant boundary term. In particular, this is true for the Holst action, which forms a heuristic basis for the “new” (EPRL/FK) spinfoam model [8, 9]. It is therefore interesting to see whether the imaginary action (2.1) makes an appearance in the new spinfoams. As the signature flips that lead to an imaginary action are a crucially Lorentzian feature, we focus on the Lorentzian spinfoam model.

Since the model is based on an action formula only heuristically, we must look at its output, i.e. at the transition amplitudes. In a classical limit, the logarithm of a quantum amplitude (divided by  $i$ ) acquires the meaning of an action:  $\ln A \rightarrow iS$ . In the spinfoam model, a simplified semiclassical analysis can be performed by considering geometries with very large discrete elements, i.e. with spins  $j \gg 1$  on the spinfoam faces. One can then consider coherent boundary states peaked on specific values of the intrinsic metric and extrinsic curvature (which are non-commuting variables) [32]. A useful middle ground are so-called “semi-coherent” boundary states, which were studied in [33]. These are similar to fully-coherent states, but have definite values for the areas, i.e. for the spins  $j$ .

---

<sup>4</sup>We are focusing here on the bulk term. A similar argument can be made for the boundary term.

## 4.2 The 4-simplex spinfoam action for large spins

In [33], Barrett et.al. studied the spinfoam vertex amplitude  $f_4$  for a large-spin semi-coherent boundary state describing a flat 4-simplex - the simplest non-trivial polytope in spacetime. The boundary is composed of five spacelike tetrahedra, intersecting at ten triangles. For boundary data that yields a consistent 4-simplex geometry, the authors of [33] reduced the vertex amplitude to a sum of two saddle-point contributions. The two saddle points describe two configurations of the 4-simplex related by parity (or time reversal). A fully coherent boundary state that includes a smearing over spins picks out one of these saddle points [32]. Taking this into account, we write the result of [33] as:

$$f_4 \rightarrow (-1)^x N_{\pm} e^{iS_{\pm}} , \quad (4.1)$$

where the sign in the subscripts distinguishes the two saddle points. The sign factor  $(-1)^x$  arises from the combinatorics of the boundary graph. The coefficients  $N_{\pm}$  are “weak” functions of the boundary data, i.e. their contribution to  $\ln f_4$  is negligible (in [34], numerical evidence was given to the effect that  $N_+$  and  $N_-$  are complex conjugates). Thus, we have  $\ln f_4 \rightarrow iS_{\pm}$ , so that the quantity  $S_{\pm}$  has the usual meaning of action. On this point, we deviated from the notation in [33]: there, the exponent in (4.1) is itself called an “action”. This means that our action differs from that in [33] by a factor of  $i$ . With this difference in mind, the result of [33] for  $S_{\pm}$  reads:

$$S_{\pm} = \sum_l j_l (\pm \gamma \Theta_l - \Pi_l) . \quad (4.2)$$

Here, we kept the second term, which in [33] was taken outside the exponent  $e^{iS_{\pm}}$ . The reason for this will become clear below.  $\gamma$  in (4.2) is the Barbero-Immirzi parameter. The sum is over the links in the boundary spin-network, or, equivalently, the faces of the spinfoam. Geometrically, they correspond to the triangular 2d faces of the 4-simplex. Each of these faces is a “corner”, in the sense that two boundary hypersurfaces (in this case, tetrahedral hyperfaces) intersect there at an angle. The  $j_l$  are spin variables which are proportional to the triangle areas  $A_l$ . We will elaborate on the precise nature of this proportionality below. Eq. (4.2) is derived in the limit  $j_l \gg 1$ . The  $\Theta_l$  are the boost angles between the pairs of tetrahedra intersecting at each triangle. Let  $n_1^{\mu}$  and  $n_2^{\mu}$  be the timelike unit normals to the pair of tetrahedra intersecting at the triangle  $l$ . We choose  $n_1^{\mu}$  and  $n_2^{\mu}$  to be both ingoing with respect to the 4-simplex (taking into account the timelike signature, this gives the normals a positive scalar product with outgoing vectors [2]). The angle  $\Theta_l$  is then defined by:

$$\Theta_l = \begin{cases} -\operatorname{acosh}(-n_1 \cdot n_2) & n_1 \cdot n_2 < 0 \quad (\text{thick corner}) \\ +\operatorname{acosh}(+n_1 \cdot n_2) & n_1 \cdot n_2 > 0 \quad (\text{thin corner}) \end{cases} . \quad (4.3)$$

Here, a “thick corner” is one where both normals  $n_1^{\mu}, n_2^{\mu}$  have the same time orientation, while a “thin corner” is one where the time orientations are opposite. See figure 3. Finally, the  $\Pi_l$  in (4.2) are defined as:

$$\Pi_l = \begin{cases} 0 & \text{thick corner} \\ \pi & \text{thin corner} \end{cases} . \quad (4.4)$$

Let us now return to the proportionality between the spins  $j_l$  in (4.2) and the triangle areas  $A_l$ . It is given by:

$$A_l = 8\pi G \operatorname{sign}(\gamma) \gamma j_l , \quad (4.5)$$

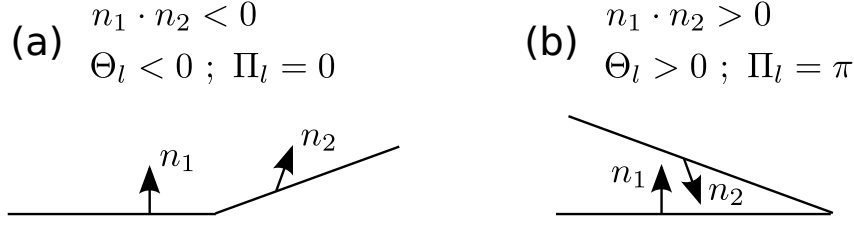


Figure 3: Two types of corners between spacelike tetrahedra: thick (a) and thin (b). The arrows denote ingoing unit normals. These correspond to outgoing covectors, i.e. have a positive scalar product with outgoing vectors. For each type of corner, the content of eqs. (4.3)-(4.4) is summarized.

where we keep in mind that  $\gamma$  can have either sign, while the areas  $A_l$  must be positive. We refrain from replacing  $\text{sign}(\gamma)\gamma \rightarrow |\gamma|$ , since that would interfere with the analytical continuation below. Substituting (4.5) into (4.2), the action becomes:

$$S_{\pm} = \frac{\text{sign}(\gamma)}{8\pi G} \sum_l A_l \left( \pm \Theta_l - \frac{\Pi_l}{\gamma} \right) . \quad (4.6)$$

### 4.3 The classical action for a 4-simplex

For comparison, let us now find the classical GR action for a flat 4-simplex, including the imaginary part described in [1, 2]. Having shown that the different classical actions agree on-shell up to signs, we will use for this purpose the second-order action (3.1):

$$S_{\text{2nd-order}} = \frac{1}{16\pi G} \int_{\Omega} \sqrt{-g} R d^d x + \frac{1}{8\pi G} \int_{\partial\Omega} \sqrt{\frac{-h}{n \cdot n}} K d^{d-1} x . \quad (4.7)$$

While the Holst action (3.21) is more closely related to the spinfoam model, we cannot use it directly in our comparison. This is because of the sensitivity of (3.21) to the sign of  $\det e$ , which has no direct counterpart in the spinfoam variables. As we will discuss in section 4.4, one can say that the spinfoam result (4.6) retains the dependence on  $\text{sign}(\det e)$  through the  $\pm$  sign that distinguishes the two saddle points.

Since we are in flat spacetime, the bulk term in (4.7) vanishes. The boundary's extrinsic curvature, and with it the York-Gibbons-Hawking boundary term, is concentrated on the 2d triangular corners. We evaluate these corner terms according to the recipe in [2]. At each corner, we consider the normals to the two intersecting tetrahedra, depicted in figure 3. Each normal can be assigned an angle (actually, a boost parameter) in the 1+1d plane orthogonal to the corner triangle. To cover more than one quadrant of the Lorentzian plane, the angles are necessarily complex. The absolute value of the angles' real part is described as usual by hyperbolic functions. The sign and the imaginary part are depicted in figure 4. The corner contributions to the action are then given by:

$$S_{\text{2nd-order}} = \frac{1}{8\pi G} \sum_l \alpha_l A_l , \quad (4.8)$$

where  $A_l$  is the corner's area, and  $\alpha_l$  is the angle difference between the two normals as one travels counter-clockwise in figure 3. Comparing with eqs. (4.3)-(4.4), we find that the corner angles  $\alpha_l$  can be written as:

$$\alpha_l = -\Theta_l + i\Pi_l . \quad (4.9)$$

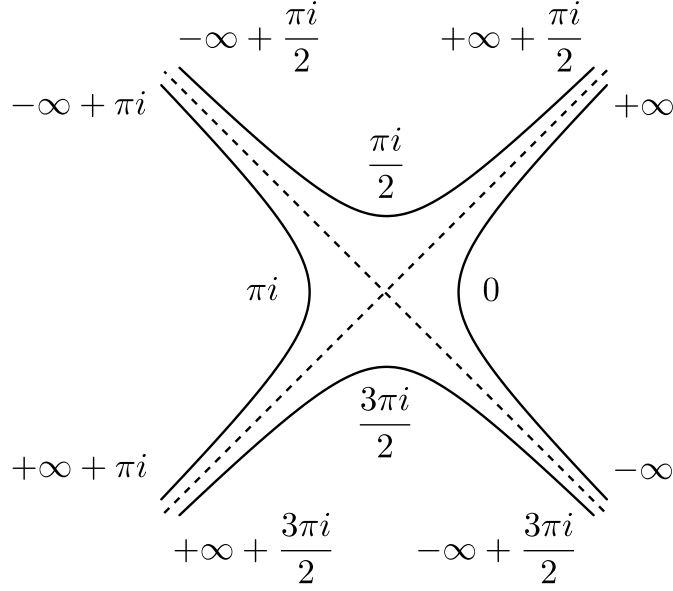


Figure 4: An assignment of boost angles to points in a Lorentzian plane. The points represent values of the boundary normal  $n^\mu$  in the 1+1d plane transverse to a corner (2d face) of the 4-simplex. The angles are defined up to integer multiples of  $2\pi i$ .

This brings the classical action (4.8) to the form:

$$S_{\text{2nd-order}} = \frac{1}{8\pi G} \sum_l A_l (-\Theta_l + i\Pi_l) . \quad (4.10)$$

#### 4.4 Comparison and analytical continuation in $\gamma$

Let us now compare the spinfoam “action” (4.6) with the classical 4-simplex action (4.10). The spinfoam formula (4.6) was derived for real values of  $\gamma$ . For such values,  $S_\pm$  are also real, and therefore cannot reproduce the complex result (4.10). For real  $\gamma$ , the  $\Pi_l$  terms sum up to an integer multiple of  $\pi$  [33], yielding a simple sign factor in the amplitude  $e^{iS_\pm}$ . As a result, in [33], the  $\Pi_l$  terms were separated from the action.

However, if we analytically continue (4.6) to complex  $\gamma$ , the  $\Pi_l$  terms can be made to reproduce the imaginary part of the classical action. The non-trivial part of the analytical continuation is the factor of  $\text{sign}(\gamma)$  in (4.6). This must be continued to a constant function, whose value depends on whether we start from  $\gamma > 0$  or from  $\gamma < 0$ . Thus, we must properly speak of two separate analytical continuations<sup>5</sup>: one from  $\gamma > 0$  with  $\text{sign}(\gamma) = 1$ , and one from  $\gamma < 0$  with  $\text{sign}(\gamma) = -1$ . With this in mind, let us analytically continue the spinfoam action  $S_\pm$  to  $\gamma = \text{sign}(\gamma)i$ . Depending on the original value of  $\text{sign}(\gamma)$ , this corresponds heuristically to a self-dual or anti-self-dual connection. Making the substitution  $\gamma \rightarrow \text{sign}(\gamma)i$  in (4.6), we get:

$$S_\pm \rightarrow \mp \text{sign}(\gamma) \text{Re } S_{\text{2nd-order}} + i \text{Im } S_{\text{2nd-order}} , \quad (4.11)$$

where  $S_{\text{2nd-order}}$  is the classical second-order action (4.10). The result (4.11) has the following properties:

<sup>5</sup>As with  $\det e$  in section 3.5, it is instructive to view the two analytical domains as arising from the function  $\sqrt{\gamma^2}$ . This is because the more basic operator in loop quantum gravity is not the area  $A_l \sim \text{sign}(\gamma)\gamma$ , but its square  $A_l^2 \sim \gamma^2$ .

1. The imaginary part coincides with that of the classical action. In particular, it is positive by construction for both saddle points, giving exponentially suppressed amplitudes  $e^{iS_{\pm}}$ .
2. The real part coincides with that of the second-order classical action (3.1), up to sign. This sign is opposite for the two saddle points.
3. The amplitudes  $e^{iS_+}$  and  $e^{iS_-}$  for the two saddle points are complex-conjugate to each other. This was also the case for real  $\gamma$ .
4. Switching the sign of  $\gamma$  corresponds to complex-conjugating  $iS_{\pm}$ . Since  $iS_+$  and  $iS_-$  are complex conjugates, this is equivalent to swapping the two saddle points.

It is plausible [29] that the two saddle-point configurations should be understood as two different values of  $\text{sign}(\det e)$ . Then the  $\mp$  sign in (4.11) reflects the fact that the real part of the on-shell first-order Holst action (3.21) changes sign together with  $\det e$ . The added dependence on  $\text{sign}(\gamma)$  in the spinfoam result is not surprising. In the spinfoam model, there is no variable corresponding to  $\det e$  directly, and the difference between left-handed and right-handed orientations enters only through  $\gamma$ . As we’ve seen, the feature of two separate analytical domains (section 3.5) also survives in the spinfoam result, but with  $\gamma$  as the relevant variable. Finally, we stress that *all* the dependence of the amplitude on  $\gamma$  is a “quantum effect”, with no counterpart in the classical on-shell action.

## 5 Discussion

In the previous sections, two main observations were made. In section 3, we’ve shown that the imaginary part of the GR action resulting from the York-Gibbons-Hawking boundary term is present also in first-order formulations. In section 4, we’ve shown that this imaginary part can also be recovered in a semi-classical analysis of the EPRL/FK spinfoam model, by analytically continuing the Barbero-Immirzi parameter  $\gamma$  to  $\pm i$  in the final result.

The original motivation for even considering this analytical continuation stems from the recent observation [16] that the Bekenstein-Hawking entropy with the correct numerical coefficient can be obtained within loop quantum gravity by a similar procedure. We comment further on this issue in section 5.3. In particular, we interpret the calculation of [16], along with our results from section 4, in the context of a “transplanckian” regime of LQG. For us, both calculations demonstrate that this regime correctly reproduces certain properties of semiclassical GR, provided that one sets  $\gamma = \pm i$ .

We stress that loop quantum gravity is well-defined only for real values of  $\gamma$ , so that it’s currently a purely formal statement to consider a complex  $\gamma$  in the quantum theory. On the other hand, an analytical continuation as the one presented could serve as an indirect definition of the theory with complex  $\gamma$ . While this may seem a suspicious procedure, it is tempting to follow it through. Indeed, self-dual variables corresponding to  $\gamma = \pm i$  have a distinguished role already in the classical theory, leading to a polynomial (density-weight two) Hamiltonian constraint.

### 5.1 The large-spin limit as a high-energy “transplanckian” regime

From the point of view of quantum field theory, Lagrangian parameters such as  $\gamma$  are expected to run under the renormalization group (RG). We’ve observed that  $\gamma$  has two limiting behaviors. In classical GR, the value of  $\gamma$  is arbitrary, and has no effect on the action. On the other hand, in the large-spin limit of the spinfoam model,  $\gamma$  must take the values  $\pm i$  for the effective action



to have the correct GR-like behavior, in particular the correct imaginary part. This leads us to suspect a sort of RG flow between the two regimes. To make this statement more precise, we must understand what is meant by the large-spin limit.

Before anything else, the large-spin limit of LQG is a mathematical structure. As such, it may enter physics in different contexts. In the spinfoam literature, the large-spin limit is often referred to as “the” semiclassical limit of LQG, with the implication that it produces the classical continuum GR that we observe at large distances. In this picture, the magnitude of the spins defines a mesoscopic scale, set between the Planck scale and the scale of continuum wavelengths that one wishes to describe. At this mesoscopic scale, some set of observables, e.g. areas and angles in Regge gravity, takes the values of a chosen classical geometry, with small relative uncertainties. The continuum emerges from adding together such semiclassical discrete elements. A similar picture emerges in the canonical framework. There, one approximates phase-space points of classical GR by coherent states on a fixed graph, with fluctuating magnitudes of the spins. One chooses a graph with sufficiently many links and nodes so that the continuum is well-approximated, but sufficiently few so that the relative uncertainties are minimized. See chapter 11 of [7] and [35] for a discussion and [36, 37, 38, 39] for original literature<sup>6</sup>. Approaches such as these are potentially valid, if one views graphs with large spins as a coarse-graining of finer graphs with small spins, in a spirit similar to RG flow. However, the details of such a coarse-graining procedure, in particular the link between  $j \sim 1$  and  $j \gg 1$ , are not well-understood.

We in this section will consider “the” large-spin limit in a more straightforward context - as the special subset of states in the fundamental theory that happen to have large spin labels. There is no coarse-graining implied. In particular, the couplings  $G$  and  $\gamma$  are the same as those in the fundamental theory (which need not be the case in the coarse-graining picture). The “classical GR” that this limit reproduces is a discretized version of the GR that was quantized to obtain LQG. This is not the same as the observed GR, which is meant to emerge through coarse-graining.

Indeed, we’ve already noted two differences between the two “classical GR’s”. The observed GR lives in the continuum and is not sensitive to  $\gamma$ . In contrast, the GR of the large-spin limit is discrete (like Regge gravity) and sensitive to  $\gamma$  (unlike Regge gravity). Thus, we view the effective action at large spins as distinct from the action of the observed, continuum GR. Therefore, the requirement for the large-spin effective action to have the correct classical form (4.10) does not really follow from consistency with the continuum theory. Instead, we see it as a consistency check on the quantization procedure itself.

What, then, is the physical meaning of this non-coarse-grained large-spin limit? Clearly, it describes the interaction of very large “atoms of space”. In quantum gravity, a large geometric size may arise both in a low-energy context (a large wavelength) and in a high-energy context (a large Schwarzschild radius). Here, “low-energy” and “high-energy” should be understood as much lower or much higher than the Planck scale, which (for finite  $\gamma$ ) is the natural scale of LQG. We argue that the large distances associated with large spins should be viewed in a *high-energy* context. Indeed, long wavelengths with low energy imply a perturbation over a background spacetime. In contrast, a large-spin state in LQG *determines* the structure of spacetime, much like a heavy black hole. This is further supported by the picture of LQG intertwiners as miniature “quantum black holes” [45]. In that picture, large spins imply a large

---

<sup>6</sup>The usual caveats of using coherent states apply: only a chosen subalgebra of classical observables can be approximated, and the coherent states must be geared to that subalgebra. A systematic construction principle is however provided by the complexifier method [40]. Dynamical stability of coherent states is unknown for non-linear systems like GR. This point is especially important in the context of quantum gravity, since one would like to prove the dynamical stability of e.g. Minkowski space. In the diff-invariant context, further technical complications appear such as graph-changing operators and constraints, leading to the algebraic quantum gravity program [41, 42, 43, 44].

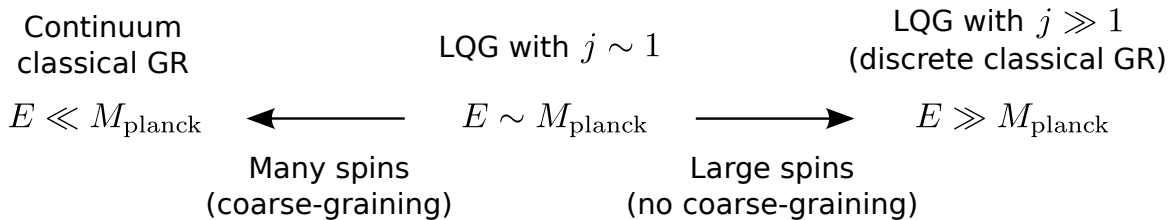


Figure 5: Two classical-GR limits of loop quantum gravity. At high energy, discrete classical geometries are described by coherent states with large spins (no coarse graining implied). At low energy, continuum classical geometries are supposed to emerge through coarse graining.

“black hole”, and therefore high energy in the sense of a large “Schwarzschild radius”.

In this way, we arrive at a picture of the large-spin limit as the regime where atoms of space with transplanckian energy interact. In particle-physics terms, the analogous situation is a scattering process of two particles with center-of-mass energy  $E \gg M_{\text{planck}}$ . The large-spin limit corresponds to the early stages of such a process, before the energy is dissipated into light degrees of freedom. After this dissipation, it is believed that the state should be viewed as a classical black hole, following the rules of the observed classical GR (see e.g. [46]). Before the dissipation, properly transplanckian physics takes place. There is no a-priori reason that this physics should be described by anything resembling GR. In LQG (as opposed to string theory), the fundamental theory is a quantization of GR *by assumption*. As a result, through the mechanism of coherent states with large quantum numbers, fundamental transplanckian processes *are* described by a (discrete) classical-GR limit. However, we stress again that this is not the same limit as the continuum GR describing classical gravity in the observed world. We stress also that the large-spin limit is “transplanckian” only in the sense of high energies, not in the sense of small distances. Degrees of freedom that are transplanckian in both senses at once are very likely ruled out on general grounds [46].

We conclude that the two classical GR's are in fact two *opposite* putative limits of the quantum theory, in terms of the energies of the quanta involved. The observed continuum GR corresponds to a low-energy “IR regime” of subplanckian quanta (gravitons). The discrete classical GR of the large-spin limit corresponds to a high-energy “UV regime” of transplanckian quanta (spins and intertwiners). The situation is summarized in figure 5. It is somewhat analogous to the situation in QCD, which becomes two different free theories in the UV and in the IR (a theory of quarks and gluons in the former, and a theory of pions in the latter).

## 5.2 The running of $\gamma$

A coherent picture now emerges with respect to the running of  $\gamma$ . In the IR, the continuum GR is insensitive to the value of  $\gamma$ . In the UV, the discrete GR of the large-spin limit prefers  $\gamma = \pm i$ . This suggests that  $\gamma$  “runs” from an arbitrary value in the IR to a UV fixed point. We stress that this “running” is not necessarily well-defined at the intermediate, Planck-scale energies. In the regime where individual spins are both small and relevant, it is quite possible that the dynamics is not described by any GR-like effective action.

Interestingly, a similar picture for the flow of  $\gamma$  was recently obtained in a very different framework. In [15], Benedetti and Speziale studied the 1-loop running of  $\gamma$  in effective field theory for the Holst action with a minimally coupled fermion. The calculation was done in a Euclidean framework, where the self-dual connection corresponds to  $\gamma = \pm 1$  rather than  $\gamma = \pm i$ . It was found that  $\gamma$  runs from an arbitrary initial value in the subplanckian IR to the self-dual value  $\pm 1$  in the transplanckian UV. It is tempting to analytically continue this statement to the

Lorentzian, saying that  $\gamma$  runs from an arbitrary IR value to  $\pm i$  in the UV.

This convergence between the perturbative picture and the one suggested by large-spin amplitudes is exciting, and indeed motivated our reasoning in section 5.1. Nevertheless, some obvious caveats should be mentioned. First, we stress again that we cannot directly make sense of a quantum theory with complex  $\gamma$ , be it in a perturbative framework or in LQG. Second, the perturbative running cannot really be trusted beyond the Planck energy. At best, it is suggestive of what should happen at transplanckian energies, with the suggestion borne out by the large-spin limit of LQG. Finally, we should note that contradictory results for the running of  $\gamma$  in pure GR have been obtained in [15] in a 1-loop perturbative calculation, as well as in [47, 48] in the asymptotic safety framework. However, those results refer to gauge-dependent quantities, and their significance is not clear to us.

A last comment concerning the running is in order. As observed in section 3.4,  $\gamma$  appears in the classical action as the prefactor of a combination of the Holst modification and the Nieh-Yan density. In other words, when demanding a well-defined variational principle, it is not valid to use either the Holst modification or the Nieh-Yan density individually. This point is important because one could object when that using the Nieh-Yan density as a modification for the Palatini action, the Barbero-Immirzi parameter would not run due to the topological nature of the Nieh-Yan density. This issue is also discussed from a different perspective in [15].

### 5.3 Black hole entropy at large spins with $\gamma = \pm i$

The black hole entropy calculation proposed in [16] has been our initial motivation for considering the substitution  $\gamma = \pm i$  in the large-spin formula (4.6). In [16], the authors propose to compute the black hole entropy within LQG in the large-spin limit by fixing the number of spin-network punctures on the horizon and setting  $\gamma$  to  $\pm i$ . As a result, the formula for the dimension of the Chern-Simons theory describing the horizon obtains a dominant term, and the resulting entropy is given by  $A/4G$ . Another work in this vein is [17], where the authors studied an LQG quantization of GR conformally coupled to a scalar field. There, one can count states resulting from a classical gauge-fixing of the Hamiltonian constraint. The entropy of these states comes out with a wrong dependency on the scalar field, unless one employs the reasoning of [16] and chooses  $\gamma$  to reflect the self-dual case.

The calculation in [16] is conceptually different from previous entropy calculations in LQG, see e.g. [49]. The main difference is that in [16], one fixes the number of punctures. From the perspective of a continuum GR limit (the low-energy “IR limit” of section 5.1), one would expect instead to sum over all spin-network configurations with a given total area. It then follows that graphs with small spins dominate the entropy [49]. On the other hand, in the high-energy “UV limit” from section 5.1, it is natural to construct a “black hole” from a limited number of large area elements. Of course, this object does not coincide with what is usually meant by a black hole in continuum GR. However, it is the natural “transplanckian” analogue, given the interpretation of a continuum black hole as a large intertwiner [45]. We note that the “transplanckian” black hole should be viewed as a temporary state: with time, it should thermalize into a continuum black hole, which in LQG will be described by many small spins. It is thus conceptually similar to the early stages of a particle collision with transplanckian center-of-mass energy.

Since the “transplanckian” black hole does not correspond to the continuum GR limit, there is also no need for its entropy to coincide with what is usually referred to as the Bekenstein-Hawking entropy. In fact, the entropy derived in [16, 17] is  $A/4G$  in terms of the *high*-energy Newton’s constant, i.e. the bare Newton’s constant  $G$  from the definition of LQG. This entropy is in agreement with what one would expect from the effective (discrete) GR action in the “transplanckian” large-spin limit of spinfoams, which is given in terms of the same  $G$ . In

contrast, the usual Bekenstein-Hawking entropy is given in terms of the effective low-energy  $G$  of the continuum theory. There is no a priori reason why the Newton's constants in the two different classical limits should coincide.

The entropy calculation proposed in [16] should thus be interpreted within the “transplanckian” regime. This is in contrast to the previous calculations such as [49], which aim at the continuum limit<sup>7</sup>. The two main assumptions of [16], i.e. setting  $\gamma$  to  $\pm i$  and considering a fixed number of spins, seem to make sense only in the “transplanckian” context, where they agree with the independent results from spinfoam asymptotics and from perturbative calculations. We stress again that setting  $\gamma$  to  $\pm i$  is a purely formal statement at the moment, since it is currently unknown how to formulate LQG properly with non-real  $\gamma$ .

#### 5.4 $\gamma \rightarrow \pm i$ as a result of coarse graining?

As argued above, setting  $\gamma$  to  $\pm i$  for large spins has an interpretation as a “transplanckian” limit in the sense of large Schwarzschild radii. Now, the natural question arises whether setting  $\gamma$  to  $\pm i$  could also have an interpretation in terms of a (to be understood) coarse graining procedure. While we are not aware of direct arguments leading to this conclusion, we want to remark that all the above observations are also consistent with the coarse graining picture in the following (more or less vague) sense: in the coarse graining picture, the correct physical result is obtained by performing the calculation for arbitrary real  $\gamma$  in the large spin limit and sending  $\gamma$  to  $\pm i$  after all calculations have been performed. This is especially attractive for the black hole entropy calculation, because a fixed number of (large spin) punctures would already incorporate, by the definition of coarse graining, all possible subdivisions into small spins. It is however unclear to us how sending  $\gamma$  to  $\pm i$  could result from a coarse graining procedure.

## 6 Conclusion

In this paper, we built on the recent observation that the second-order GR action for bounded regions has an imaginary part. We established that the same imaginary part is present also in first-order formulations of gravity. It was then shown that this imaginary part can be recovered from the large-spin asymptotics of the EPRL/FK spinfoam model, by analytically continuing the result from real Barbero-Immirzi parameter  $\gamma$  to  $\gamma = \pm i$ . We proposed to view this limit as a “transplanckian” regime of LQG, in the sense of high energies but not of small distances. We argued that it's natural for the effective action in this regime to describe a discretized version of GR, governed by the high-energy Newton's constant. Further evidence for this point of view coming from a perturbative calculation and black hole entropy calculations has been discussed. While the calculations in sections 3 and 4 are robust, the arguments in the discussion section 5 are more intuitive and should be taken with due care. Again, especially statements about the running of  $\gamma$  to  $\pm i$  in full Lorentzian LQG are only formal, since the quantum theory is ill-defined for non-real  $\gamma$ .

## Acknowledgements

NB and YN were supported by the NSF Grant PHY-1205388 and the Eberly research funds of The Pennsylvania State University. We thank Abhay Ashtekar for helpful discussions and

---

<sup>7</sup>It has been argued that the Barbero-Immirzi parameter can be fixed via black hole entropy calculations such as [49]. This however does not seem to be the case, as newer results show [50, 51]. In particular, one would need to compare the result of, e.g. [49], with an effective continuum action derived in a proper coarse-graining procedure.

Andreas Thurn for useful comments on a draft of this article.

## References

- [1] Y. Neiman, “On-shell actions with lightlike boundary data,” [arXiv:1212.2922 \[hep-th\]](#).
- [2] Y. Neiman, “The imaginary part of the gravity action and black hole entropy,” [arXiv:1301.7041 \[gr-qc\]](#).
- [3] J. W. York, “Role of Conformal Three-Geometry in the Dynamics of Gravitation,” *Physical Review Letters* **28** (1972) 1082–1085.
- [4] G. W. Gibbons and S. W. Hawking, “Action integrals and partition functions in quantum gravity,” *Physical Review D* **15** (1977) 2752–2756.
- [5] A. Ashtekar, J. Engle, and D. Sloan, “Asymptotics and Hamiltonians in a first-order formalism,” *Classical and Quantum Gravity* **25** (2008) 095020, [arXiv:0802.2527 \[gr-qc\]](#).
- [6] C. Rovelli, *Quantum Gravity*. Cambridge University Press, Cambridge, 2004.
- [7] T. Thiemann, *Modern Canonical Quantum General Relativity*. Cambridge University Press, Cambridge, 2007.
- [8] L. Freidel and K. Krasnov, “A new spin foam model for 4D gravity,” *Classical and Quantum Gravity* **25** (2008) 125018, [arXiv:0708.1595 \[gr-qc\]](#).
- [9] J. Engle, E. R. Livine, R. Pereira, and C. Rovelli, “LQG vertex with finite Immirzi parameter,” *Nuclear Physics B* **799** (2008) 136–149, [arXiv:0711.0146 \[gr-qc\]](#).
- [10] A. Perez, “The Spin Foam Approach to Quantum Gravity,” [arXiv:1205.2019 \[gr-qc\]](#).
- [11] S. Holst, “Barbero’s Hamiltonian derived from a generalized Hilbert-Palatini action,” *Physical Review D* **53** (1996) 5966–5969, [arXiv:gr-qc/9511026](#).
- [12] A. Ashtekar, “New Variables for Classical and Quantum Gravity,” *Physical Review Letters* **57** (1986) 2244–2247.
- [13] J. Barbero, “Real Ashtekar variables for Lorentzian signature space-times,” *Physical Review D* **51** (1995) 5507–5510, [arXiv:gr-qc/9410014](#).
- [14] S. Mercuri, “Fermions in the Ashtekar-Barbero connection formalism for arbitrary values of the Immirzi parameter,” *Physical Review D* **73** (2006) 084016, [arXiv:gr-qc/0601013](#).
- [15] D. Benedetti and S. Speziale, “Perturbative quantum gravity with the Immirzi parameter,” *Journal of High Energy Physics* **2011** (2011) 1–31, [arXiv:1104.4028 \[hep-th\]](#).
- [16] E. Frodden, M. Geiller, K. Noui, and A. Perez, “Black Hole Entropy from complex Ashtekar variables,” [arXiv:1212.4060 \[gr-qc\]](#).
- [17] N. Bodendorfer, A. Stottmeister, and A. Thurn, “Loop quantum gravity without the Hamiltonian constraint,” *Classical and Quantum Gravity* (2013) (to appear), [arXiv:1203.6525 \[gr-qc\]](#).
- [18] S. W. Hawking, “Black hole explosions?,” *Nature* **248** (1974) 30–31.



- [19] R. Myers, “Higher-derivative gravity, surface terms, and string theory,” *Physical Review D* **36** (1987) 392–396.
- [20] T. Jacobson and G. Kang, “Increase of black hole entropy in higher curvature gravity,” *Physical Review D* **52** (1995) 3518–3528, [arXiv:gr-qc/9503020](#).
- [21] R. Arnowitt, S. Deser, and C. W. Misner, “The dynamics of general relativity,” in *Gravitation: An introduction to current research* (L. Witten, ed.), (New York), pp. 227–265, Wiley, 1962. [arXiv:gr-qc/0405109](#).
- [22] E. Dyer and K. Hinterbichler, “Boundary terms, variational principles, and higher derivative modified gravity,” *Physical Review D* **79** (2009) 024028, [arXiv:0809.4033 \[gr-qc\]](#).
- [23] P. Peldan, “Actions for gravity, with generalizations: A Review,” *Classical and Quantum Gravity* **11** (1994) 1087–1132, [arXiv:gr-qc/9305011](#).
- [24] J. B. Hartle and R. Sorkin, “Boundary terms in the action for the Regge calculus,” *General Relativity and Gravitation* **13** (1981) 541–549.
- [25] C. Rovelli and T. Thiemann, “The Immirzi parameter in quantum general relativity,” *Physical Review D* **57** (1998) 1009–1014, [arXiv:gr-qc/9705059](#).
- [26] G. Immirzi, “Quantum gravity and Regge calculus,” *Nuclear Physics B - Proceedings Supplements* **57** (1997) 65–72, [arXiv:gr-qc/9701052](#).
- [27] S. Mercuri, “A possible topological interpretation of the Barbero-Immirzi parameter,” [arXiv:0903.2270 \[gr-qc\]](#).
- [28] G. Date, R. Kaul, and S. Sengupta, “Topological interpretation of Barbero-Immirzi parameter,” *Physical Review D* **79** (2009) 044008, [arXiv:0811.4496 \[gr-qc\]](#).
- [29] C. Rovelli and E. Wilson-Ewing, “Discrete symmetries in covariant loop quantum gravity,” *Physical Review D* **86** (2012) 064002, [arXiv:1205.0733 \[gr-qc\]](#).
- [30] J. Engle, “A spin-foam vertex amplitude with the correct semiclassical limit,” [arXiv:1201.2187 \[gr-qc\]](#).
- [31] J. Engle, “A proposed proper EPRL vertex amplitude,” [arXiv:1111.2865 \[gr-qc\]](#).
- [32] E. Bianchi and Y. Ding, “Lorentzian spinfoam propagator,” *Physical Review D* **86** (2012) 104040, [arXiv:1109.6538 \[gr-qc\]](#).
- [33] J. W. Barrett, R. J. Dowdall, W. J. Fairbairn, F. Hellmann, and R. Pereira, “Lorentzian spin foam amplitudes: graphical calculus and asymptotics,” *Classical and Quantum Gravity* **27** (2010) 165009, [arXiv:0907.2440 \[gr-qc\]](#).
- [34] Y. Neiman, “Parity and reality properties of the EPRL spinfoam,” *Classical and Quantum Gravity* **29** (2012) 065008, [arXiv:1109.3946 \[gr-qc\]](#).
- [35] H. Sahlmann, T. Thiemann, and O. Winkler, “Coherent states for canonical quantum general relativity and the infinite tensor product extension,” *Nuclear Physics B* **606** (2001) 401–440, [arXiv:gr-qc/0102038](#).
- [36] T. Thiemann, “Gauge field theory coherent states (GCS): I. General properties,” *Classical and Quantum Gravity* **18** (2001) 2025–2064, [arXiv:hep-th/0005233](#).

- [37] T. Thiemann and O. Winkler, “Gauge field theory coherent states (GCS): II. Peakedness properties,” *Classical and Quantum Gravity* **18** (2001) 2561–2636, [arXiv:hep-th/0005237](#).
- [38] T. Thiemann and O. Winkler, “Gauge field theory coherent states (GCS): III. Ehrenfest theorems,” *Classical and Quantum Gravity* **18** (2001) 4629–4681, [arXiv:hep-th/0005234](#).
- [39] T. Thiemann and O. Winkler, “Gauge field theory coherent states (GCS): IV. Infinite tensor product and thermodynamical limit,” *Classical and Quantum Gravity* **18** (2001) 4997–5053, [arXiv:hep-th/0005235](#).
- [40] T. Thiemann, “Complexifier coherent states for quantum general relativity,” *Classical and Quantum Gravity* **23** (2006) 2063–2117, [arXiv:gr-qc/0206037](#).
- [41] K. Giesel and T. Thiemann, “Algebraic quantum gravity (AQG): I. Conceptual setup,” *Classical and Quantum Gravity* **24** (2007) 2465–2497, [arXiv:gr-qc/0607099](#).
- [42] K. Giesel and T. Thiemann, “Algebraic quantum gravity (AQG): II. Semiclassical analysis,” *Classical and Quantum Gravity* **24** (2007) 2499–2564, [arXiv:gr-qc/0607100](#).
- [43] K. Giesel and T. Thiemann, “Algebraic quantum gravity (AQG): III. Semiclassical perturbation theory,” *Classical and Quantum Gravity* **24** (2007) 2565–2588, [arXiv:gr-qc/0607101](#).
- [44] K. Giesel and T. Thiemann, “Algebraic quantum gravity (AQG): IV. Reduced phase space quantization of loop quantum gravity,” *Classical and Quantum Gravity* **27** (2010) 175009, [arXiv:0711.0119 \[gr-qc\]](#).
- [45] K. Krasnov and C. Rovelli, “Black holes in full quantum gravity,” *Classical and Quantum Gravity* **26** (2009) 245009, [arXiv:0905.4916 \[gr-qc\]](#).
- [46] G. Dvali, S. Folkerts, and C. Germani, “Physics of trans-Planckian gravity,” *Physical Review D* **84** (2011) 024039, [arXiv:1006.0984 \[hep-th\]](#).
- [47] J.-E. Daum and M. Reuter, “Running Immirzi Parameter and Asymptotic Safety,” [arXiv:1111.1000 \[hep-th\]](#).
- [48] J.-E. Daum and M. Reuter, “Einstein-Cartan gravity, Asymptotic Safety, and the running Immirzi parameter,” [arXiv:1301.5135 \[hep-th\]](#).
- [49] A. Ashtekar, J. Baez, and K. Krasnov, “Quantum Geometry of Isolated Horizons and Black Hole Entropy,” *Advances in Theoretical and Mathematical Physics* **4** (2000) 1–94, [arXiv:gr-qc/0005126](#).
- [50] J. Engle, K. Noui, A. Perez, and D. Pranzetti, “Black hole entropy from an SU(2)-invariant formulation of Type I isolated horizons,” *Physical Review D* **82** (2010) 044050, [arXiv:1006.0634 \[gr-qc\]](#).
- [51] A. Ghosh and A. Perez, “Black Hole Entropy and Isolated Horizons Thermodynamics,” *Physical Review Letters* **107** (2011) 241301, [arXiv:1107.1320 \[gr-qc\]](#).